Hindawi
Advances in Astronomy
Volume 2019, Article ID 6324901, 17 pages
https://doi.org/10.1155/2019/6324901

Research Article

Initial Parameter Analysis about Resonant Orbits in Earth-Moon System

Li-Bo Liu, Ying-Jing Qian, and Xiao-Dong Yang

Beijing Key Laboratory of Nonlinear Vibrations and Strength of Mechanical Structures, College of Mechanical Engineering, Beijing University of Technology, Beijing 100124, China

Correspondence should be addressed to Ying-Jing Qian; candiceqyj@163.com

Received 17 September 2018; Revised 27 November 2018; Accepted 26 December 2018; Published 23 January 2019

Academic Editor: Geza Kovacs

The initial parameters about resonant orbits in the Earth-Moon system were investigated in this study. Resonant orbits with different ratios are obtained in the two-body problem and planar circular restricted three-body problem (i.e., PCRTBP). It is found that the eccentricity and initial phase are two important initial parameters of resonant orbits that affect the closest distance between the spacecraft and the Moon. Potential resonant transition or resonant flyby may occur depending on the possibility of the spacecraft approaching the Moon. Based on an analysis of ballistic capture and flyby, the Kepler energy and the planet's perturbed gravitational sphere are used as criteria to establish connections between the initial parameters and the possible "steady" resonant orbits. The initial parameter intervals that can cause instability of the resonant orbits in the CRTBP are obtained. Examples of resonant orbits in 1:2 and 2:1 resonances are provided to verify the proposed criteria.

1. Introduction

Mean motion resonance is a common phenomenon that exists when there is a simple integer relationship between frequencies or periods [1, 2]. For example, Earth is in 8:13 resonance with Venus about the Sun; Io is in 2:1 resonance with Europa about Jupiter. The mean motion resonance of the Jupiter-Saturn is approximately 5:2 [3]. Research on resonant orbits for spacecraft can provide an alternative option for trajectory design and have potential to save propellant in real missions.

The two-body theory can be applied to many-body systems with only one major primary, where other primaries' gravitational influences are negligible. Many resonant orbits can be found with a resonant ratio that is equal to the ratio of the orbital periods corresponding to the bodies in resonance, such as the 3:1 mean motion resonance found in the 55 Cancri planetary system [4, 5] and the 2:1 motion resonance in the extrasolar planetary systems HD 82943 [6] and Gliese 876 [7, 8]. Interestingly, most planets locked in resonance exhibit maximum separation in that they avoid a close approach to the other primary. Man-made missions also can be designed to have a resonant orbit. The Interstellar Boundary Explorer (IBEX) spacecraft is currently in a highly elliptical orbit around Earth in a 3:1 resonance with the Moon [9]. It is important to note that IBEX's orbital apogee is also oriented to avoid the Moon. Voyatzis [10] carried out extensive numerical studies of planets trapped in 3:1 mean motion resonance. Antoniadou and Voyatzis [11] also found that the temporal evolution of the orbital elements depends on the mean motion resonances, which affects the dynamics and not vice versa. Murray and Dermott [2] summarized the perturbation equation for orbital elements in their monograph and showed significant periodic and quasi-periodic variations in the orbital elements. Therefore, the solution of the secular problem by Laplace for resonant orbits allows us to make assertions regarding the long-term stability of the solar system [12]. Laplace-Lagrange secular theory is valid for small eccentricities; i.e., without significant perturbations, resonant orbits for small eccentricities can exhibit constant resonant ratios after long-time evolution.

In the restricted three-body problem (i.e., CRTBP), some resonant orbits may also exist with resonant ratio that is *approximately* equal to the ratio of the orbital periods due to the secondary primary's significant gravitational influence [13]. To be more specific, the time required to complete a

revolution is not constant. Instead, for a m:n resonance in the circular restricted three-body problem, the spacecraft completes m orbits around the primary in approximately the same time required for the Moon to complete n revolutions. In this study, we call this type of resonant ratio a "*steady*" resonant ratio. Although the resonant ratio is not precise, those resonant orbits in the CRTBP are still closed and periodic [14]. Previous studies showed the existence of two and three dimensional resonant orbits in the Saturn system and KOI-730 system [15]. The targeting scheme, similar to that used to compute periodic orbits in the vicinity of the libration points, is widely used to calculate periodic resonant orbits. The initial vector seeds a correction scheme to target a perpendicular crossing of the x-axis in a nonlinear propagation [13]. Vaquero [16] numerically determined the orbit families for different resonant ratios and discussed the geometry feature of resonant orbits with different eccentricities. Similarly, Antoniadou [17] presented five types of resonant orbits with different resonant ratios and found that the resonant orbits with steady ratios generally had large eccentricities expect for a few special cases.

However, some resonant orbits in CRTBP are not "*lucky*" enough to complete "*steady*" resonant ratios. Anderson [18] focused on the resonant orbits with multiple loops near the secondary. Flyby is one of those interesting phenomena related to mean motion resonance in the CRTBP that involves a gravity assist maneuver, followed by escape after approaching the secondary primary [18]. They also explored their characteristics using a monodromy matrix and found that multiple flybys dramatically alter the resonant ratio [19]. What is more, observations show that some comets in resonance with Jupiter in the solar system exhibit "resonance transitions" into another resonant orbit when they were close to Jupiter [20]. A resonant transition is a phenomenon when the particle leaves one mean motion resonance and enters another after some time. A number of Jupiter comets such as Oterma exhibit a rapid transition from heliocentric orbits outside the orbit of Jupiter into heliocentric orbits inside the orbit of Jupiter, and vice versa. Koon [20] pointed out that the interior heliocentric orbit is typically close to the 3:2 resonance during resonance transition, while the exterior heliocentric orbit is near the 2:3 resonance. Therefore, we can conclude that resonant orbits might not exhibit "*steady*" resonant ratios mainly due to perturbations caused by the approaching second primary in the CRTBP. Obviously, it is important to discover and analyze the initial orbital geometry factors that affect resonant orbits and will allow resonant orbits involving an approach to the second primary.

Research on dynamical system analysis of resonance related flyby and transition offers an opportunity to focus on the connections between the initial resonant orbit parameters and the possibility of maintaining "steady" resonant ratios. In the analysis of flybys, Anderson [21] defined the flyby range and concluded that the spacecraft's trajectory is considered a typical two-body orbit when the spacecraft remains some set distance from the perturbing planet. This set distance is often referred to as the sphere of influence or the sphere of action, and its calculation has been the subject of considerable research by Laplace [22] and Tisserand [23]. With the purpose of understanding resonance transitions, Belbruno [24, 25] explained the comet's temporary capture and provided the necessary energy conditions for resonance transitions. The temporary nonpositive Kepler energy with respect to the secondary primary is called "*definition one*" for ballistic capture. Temporary ballistic capture is analogously referred to as weak capture, and resonant motion with respect to secondary primary was unstable during weak capture.

Based on the definition of ballistic capture [24, 25] and flyby range [19, 21], the Kepler energy and perturbing planet's sphere of influence are used as indices to establish connections between the initial parameters of resonant orbits and their possibilities of maintaining "steady" resonant ratios.

This study focuses purely on resonant orbits losing steady ratios and attempts to locate the parameter intervals that can cause those orbits to lose their steady ratios as the secondary primary is approached, where the Earth-Moon system is taken as an example.

The remainder of this paper is structured as follows. The basic dynamics of the two-body problem model and the CRTBP model are briefly introduced in Section 2. The basic methodology for constructing representative resonant orbit families in the two-body problem and the CRTBP are presented in Section 3. Two important initial parameters are selected during resonant family analysis. The parameter intervals that can cause those orbits to lose their stable resonant ratio as the secondary primary is approached are determined in Section 4. The connections between the initial parameters and possible weak capture and flyby are clarified. Conclusions are drawn in Section 5.

2. Equation of Motion

The two-body model and the CRTBP model are used to analyze the contributions of the Moon's gravitational influence and geometry properties on the resonant orbits in this study. Before proceeding further, the definitions of the coordinate systems are defined and illustrated in Figure 1.

J2000: The J2000 Geocentric Equatorial Coordinate System (i.e., J2000 $\boldsymbol{O}$-$\boldsymbol{X_e Y_e Z_e}$). Origin at the center of the Earth, the X-axis points to the vernal equinox at noon on January 1, 2000, the Z-axis points to the North Pole at this time, and the Y-axis completes the right-handed coordinate system.

GRC: Geocentric Rotating Coordinate System (i.e., GRC $\boldsymbol{O}$-$\boldsymbol{xyz}$). Origin at the center of the Earth, the x-axis points to the center of the Moon, the z-axis points to the instantaneous direction of the Moon's orbital angular momentum, and the y-axis completes the right-handed coordinate system.

Moon J2000: The J2000 Moon-centered Coordinate System (i.e., Moon J2000 $\boldsymbol{O}$-$\boldsymbol{X_m Y_m Z_m}$). Origin at the center of the Moon; the X_m-axis, Y_m-axis, and Z_m-axis are all parallel to the X-axis, Y-axis, and Z-axis, respectively.

In the two-body problem, the Moon is temporarily assumed to be massless and orbiting the Earth in a circular orbit with a radius equal to the lunar semimajor axis a_m. The angular velocity can be simplified as $\boldsymbol{\omega}_2=[0, 0, \sqrt{\mu_e/a_m^3}]$,

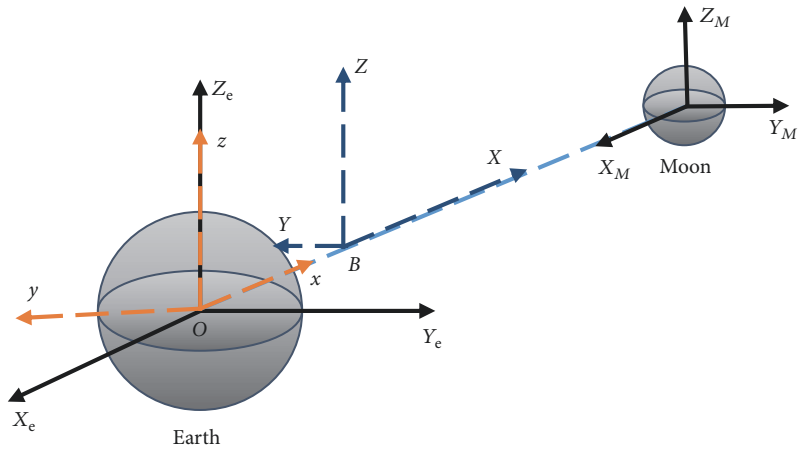

Figure 1: The J2000 coordinate system and the geocentric rotating coordinate system.

and the governing equation in the J2000 coordinate system is defined as follows:

$$\ddot{\mathbf{R}} = -\frac{\mu_e}{R^3}\mathbf{R} \tag{1}$$

where μ_e is the gravitational constant of the Earth and $\mathbf{R}$ is spacecraft's position vector in J2000.

In the CRTBP, two primaries revolve around their barycenter in circular orbits under mutual gravitational attraction. Another small particle moves into the plane defined by the two revolving primaries. The particle is considered "massless" and is attracted by the two primaries, but the motions of the primary bodies are assumed to be unaffected by the particle.

The geometry of this problem is conveniently described in GRC. In the Earth-Moon system, we define $\mu=\mu_m/(\mu_e+\mu_m)$ as the mass parameter of the three-body system. The Earth (P_1) with mass $1-\mu$ is located at (0,0,0), and the Moon (P_2) with mass μ is located at (1,0,0). The dimensionless equations of motion are

$$\begin{aligned} \ddot{X} - 2\dot{Y} &= \frac{\partial \mathbf{\Omega}}{\partial X} \\ \ddot{Y} + 2\dot{X} &= \frac{\partial \mathbf{\Omega}}{\partial Y}, \\ \ddot{Z} &= \frac{\partial \mathbf{\Omega}}{\partial Z} \end{aligned} \tag{2}$$

where $\mathbf{\Omega}$ is the pseudopotential function of the three-body problem, defined as

$$\mathbf{\Omega} = \frac{1}{2}\left((X-\mu)^2 + Y^2\right) + \frac{1-\mu}{R_1} + \frac{\mu}{R_2} + \frac{1}{2}\mu(1-\mu), \tag{3}$$

where R_1 and R_2 are the distances of the particle from P_1 and P_2, respectively:

$$\begin{aligned} R_1 &= \sqrt{X^2 + Y^2 + Z^2}, \\ R_2 &= \sqrt{(X-1)^2 + Y^2 + Z^2}. \end{aligned} \tag{4}$$

3. Resonant Orbits in the Two-Body Problem and the CRTBP

In this section, we present the basic methodology for constructing the representative resonant orbit families in the two-body problem and the CRTBP with eccentricity variations. Important geometry factors for resonant orbits that lose their *steady* resonant ratio will be found.

3.1. Resonant Orbits in the Two-Body Problem. In the two-body problem, the spacecraft is defined to be in orbital resonance with the Moon. In this peculiar case, the gravity of both the Moon and the spacecraft are neglected, and the Earth is the only gravitational source. The most straightforward approach to generate a planar resonant orbit in the two-body model is to select a set of initial parameters at periapsis. If the set of initial parameters is selected at periapsis, then the initial velocity points entirely along the y-direction. According to this definition, the initial state of a spacecraft in J2000 can be determined from the following expressions for the selected orbital elements:

$$\begin{aligned} a &= \left[\mu_e\left(\frac{T}{2\pi}\right)^2\right]^{1/3}, \\ P &= a\left(1-e^2\right), \\ R_0 &= \frac{P}{1+e\cos\theta}, \\ V_0 &= \sqrt{2\mu_e\left(\frac{1}{R_0} - \frac{1}{2a}\right)} \end{aligned} \tag{5}$$

where a is the semimajor axis, P is the semilatus rectum, R_0 is the initial distance, V_0 is the initial velocity, and θ is the true anomaly.

For simplicity we assume that the "massless" Moon moves in a circular orbit and that all motion lies in the plane of the Moon's orbit. Considering a spacecraft in an m:n resonance with the Moon, the Moon completes exactly n revolutions when the spacecraft completes m orbits about Earth. In this

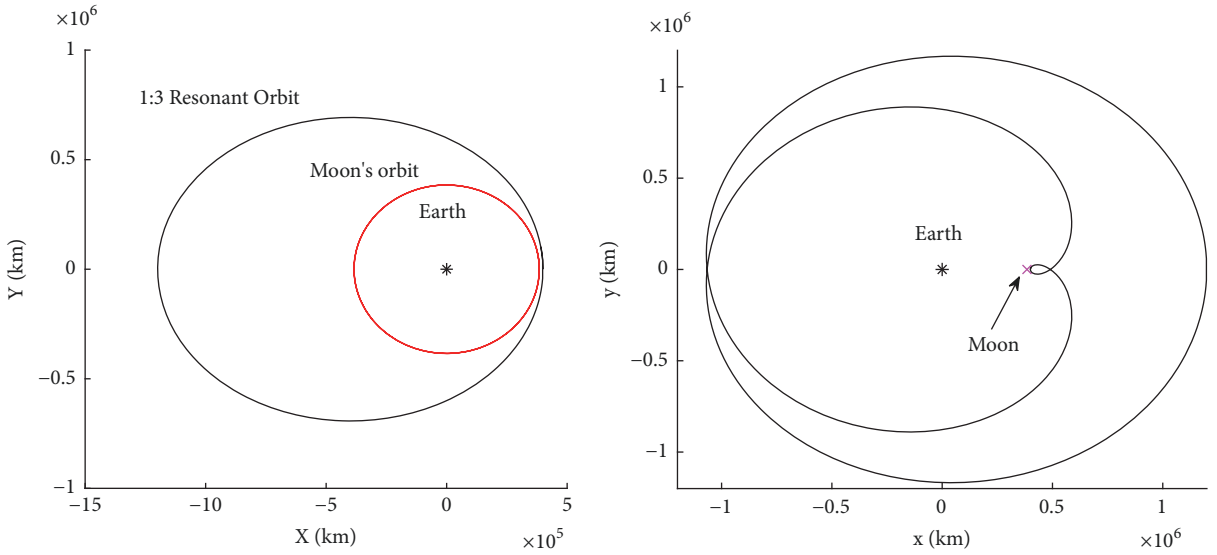

Figure 2: J2000 and GRC views of a spacecraft in a 1:3 resonant orbit with the Moon.

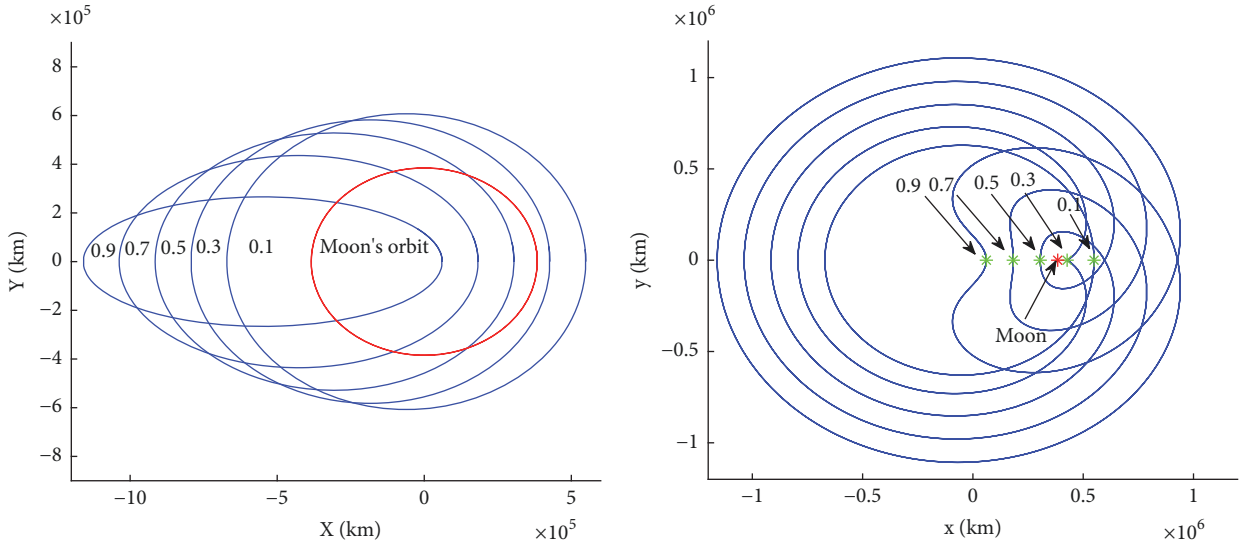

Figure 3: J2000 and GRC views of 1:2 resonant family with different eccentricities.

definition of orbital resonance, m and n are positive integers and the ratio of the orbital period of the spacecraft T to the orbital period of the Moon T_{Moon} is obtained as follows:

$$Tm = T_{Moon}n. \tag{6}$$

The orbital eccentricity is arbitrarily selected when searching for resonant orbits. Once the resonant ratio is defined, the initial state can be obtained from (5). Because the spacecraft starts from periapsis, the Earth, Moon, and spacecraft are initially collinear, and the resonant orbit can be obtained by integrating (1). The resonant family can be found with different eccentricities. The 1:3 resonant orbit is taken as an example and is illustrated in Figure 2.

(1). **Effect of Eccentricity**. The perigees of resonant orbits move toward the Earth as the eccentricity increases. The J2000 and GRC views of the 1:2 resonant family with eccentricities e = 0.1, 0.3, 0.5, 0.7, and 0.9 are shown in Figure 3. In Figure 3(a), the red trajectory is the Moon's orbit, and the blue trajectories are the 1:2 resonant orbit family. In Figure 3(b), the red point denotes the Moon in the rotating frame, and the green points are the perigees of the resonant family in the rotating frame, which are also the closest points of the resonant family to the Moon.

A special feature of resonant orbits is the formation of "loops". In Figure 3(b), we notice the 1:2 resonant orbit viewed in GRC is still elliptical without a loop when e = 0.1.

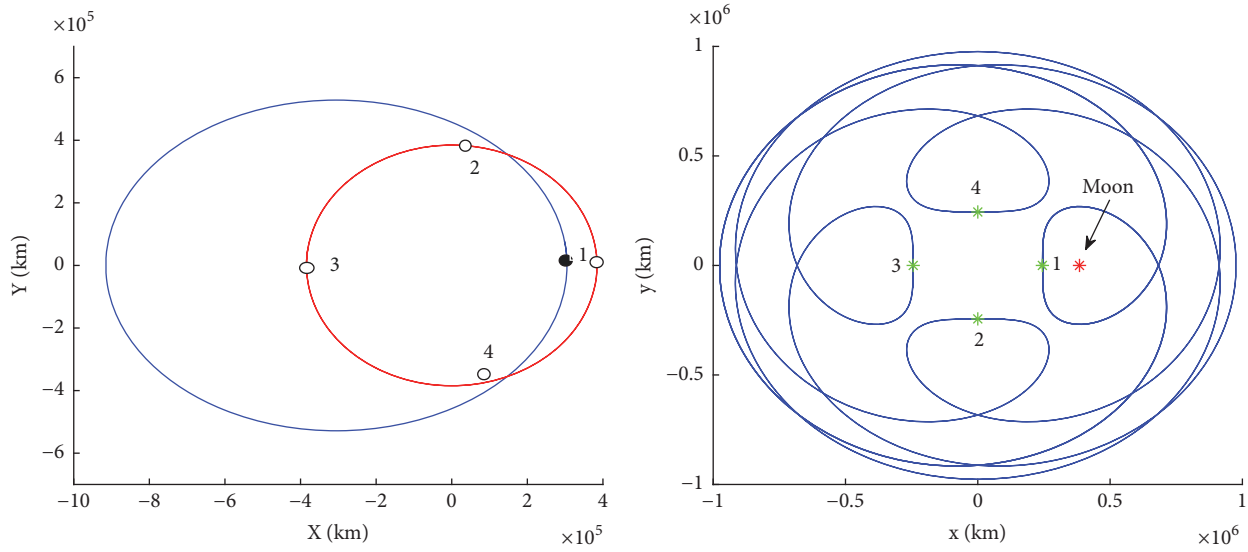

(a) J2000 view (b) GRC view

FIGURE 4: J2000 and GRC views of spacecraft in a 1:2 resonance ($e = 0.6$) with the Moon. The four initial phases between the Moon and spacecraft are $\theta_0 = 0^\circ$, 90°, 180°, and 270°.

Meanwhile, the 1:2 resonant orbits with $e = 0.3$, 0.5, 0.7, and 0.9 each form one loop in GRC. In those cases with sufficiently large eccentricity values, the angular velocity of the spacecraft at perigee is smaller than the angular velocity of the Moon. The spacecraft appears to be moving backwards in GRC. For the *m:n* resonant orbit, it takes m orbits for the spacecraft configuration to repeat itself, and the number of "loops" is always equal to m.

We also notice that resonant orbits with the same ratio have distinct views in GRC. Orbital eccentricity affects the distance between the perigee and the Moon, which will finally affect the closest distance between the spacecraft and the Moon. The spacecraft has an opportunity to approach the Moon when the eccentricity takes a certain range of values.

(2). **Effect of Initial Phase**. According to the definition of GRC, where the Moon and Earth are always fixed on the x-axis, resonant orbits with the same eccentricity are different in the GRC view when the initial phase θ_0 between Moon and spacecraft is different. Figure 4 shows the effect of the initial phase on 1:2 resonant orbits in detail. In Figure 4(a), the Moon's orbit (red trajectory) and the 1:2 resonant orbit with eccentricity $e = 0.6$ (blue trajectory) are shown in J2000. The spacecraft always starts at its perigee (denote by the black dot). Four initial phases between the Moon and the spacecraft ($\theta_0 = 0^\circ$, 90°, 180°, and 270°) are chosen. The circles marked 1, 2, 3, and 4 represent the Moon's starting position in the J2000 coordinate system. The corresponding GRC view for the four cases is shown in Figure 4(b). The orbital family will rotate clockwise as phase difference increases. The red point denotes the Moon and the green points are the closest points to the Moon along the resonant orbits. It is clear that the initial phase can dramatically alter the closest distance between spacecraft and the Moon, which also offers opportunities to approach the Moon.

One can conclude that the eccentricity and initial phase are two important initial parameters of resonant orbits that affect the closest distance between the spacecraft and the Moon. Potential weak capture or flyby may occur due to opportunities where Moon may be approached.

3.2. Resonant Orbits in the CRTBP. Based on the initial states provided from the two-body problem, the corresponding resonant orbits in the CRTBP are easily obtained from (2). The resonant orbits in the CRTBP are more complicated due to the gravitational force of Moon. The straightforward method for computing resonant orbits in the CRTBP is to modify the known solutions from the two-body problem and adapt them into the CRTBP. The initial states from the two-body problem are reasonably accurate initial estimates. A targeting scheme is required to compute closed, periodic, resonant orbits in the CRTBP.

The corrections scheme during each iteration is designed to cross the x-axis along a perpendicular direction in nonlinear propagation. The numerical integration process is forced to terminate only at the desired perpendicular crossing and restricts the location of the x-axis crossing as the stopping condition for the corrections algorithm. Detailed information regarding differential correction can be found in Vaquero [13]. The closed, periodic resonant orbit in the CRTBP model can be obtained by using the shooting method to modify the initial value five times.

For a certain resonant ratio, each resonant orbit is uniquely characterized by the eccentricity, a single-parameter continuation method is used to generate families of resonant orbits. Figures 5(a)–5(j) show a variety of dimensionless resonant orbit families in the Earth-Moon system with initial phase $\theta_0 = 0$. The magenta point in each subplot denotes the location of the Moon in GRC. The outermost trajectories

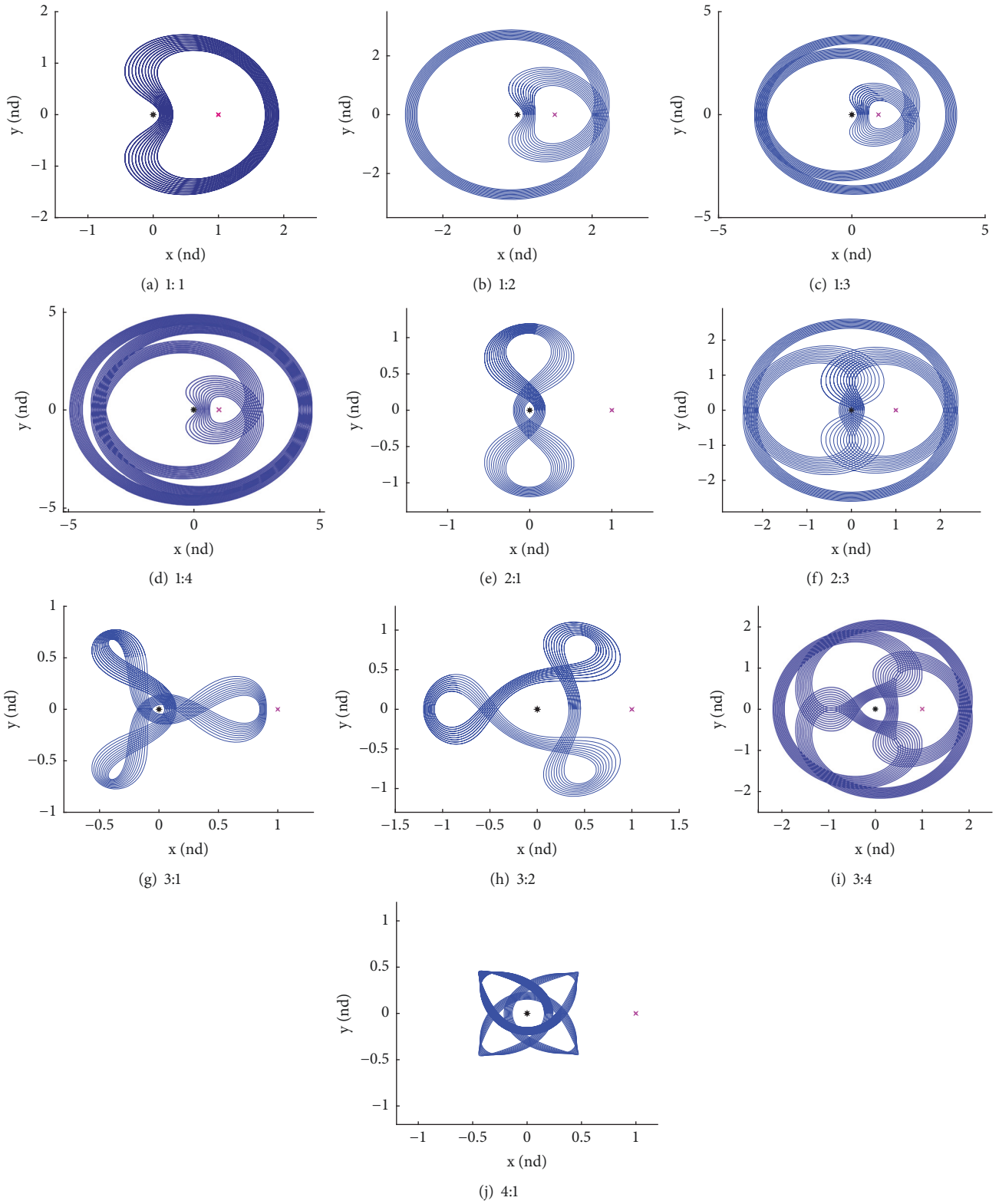

Figure 5: Resonant families in the Earth-Moon system plotted in GRC ($\theta_0 = 0$).

in each subplot in Figure 5 are the trajectories with largest eccentricities. Orbital families with 2:2, 3:3, 4:4, and 4:2 resonances are not shown in Figure 5 since they are the same as the 1:1 and 2:1 resonances in nature, respectively.

All the planar resonant orbits are symmetric across the x-axis. It is worth mentioning that the period of the resonant orbit in the CRTBP is often close to that of a selected resonance with integer ratio. The resonant orbits in the CRTBP with steady ratio generally exhibit similar characteristics as the orbits in the two-body problem. Resonant orbits with m:n ratio also have m "loops" for large eccentricity.

The simulation results show some complete resonant families within the CRTBP model in Figures 5(e), 5(g), 5(h), and 5(j). One can see in those subplots that the Moon is entirely outside the resonant family. The largest size orbits of these families in GRC are still far from Moon. In other words, there is no opportunity for a spacecraft to approach the Moon when $\theta_0 = 0^\circ$. However, as we concluded from Figure 4, the results show that the orbital family will rotate clockwise by θ_0 as θ_0 increases. Taking the 2:1 family as an example, the orbital family will rotate 90° when $\theta_0 = 90^\circ$ while the Moon remains fixed, which will offer opportunities for approaching the Moon. A detailed analysis on the effects of eccentricity and initial phase will be shown in the next section.

4. Analysis of the Initial Parameters of Resonant Orbits

An analysis of the two critical initial parameters (eccentricity and initial phase) is discussed further in this section. Connections between the initial parameters, a possible resonance transition, and flyby are established. We attempt to locate the initial parameter intervals for eccentricity e and initial phase θ_0, which may cause a spacecraft to approach the Moon and cause the resonant orbits to lose their steady ratio. This analysis will benefit trajectory design in a real mission.

Results from the literature show that successive resonant flybys can decrease or increase the orbital Kepler energy, while weak capture occurs when the Kepler energy with respect to Moon is temporarily nonpositive [20]. Clearly, the orbital Kepler energy H_2 must be considered in this study, which is defined in

$$r_2 = (x - r_m)^2 + y^2 \tag{7}$$

$$v_2^2 = (\dot{x} - \omega y)^2 + [\dot{y} + \omega (x - r_m)]^2, \tag{8}$$

$$H_2 = \frac{1}{2} v_2^2 - \frac{\mu_m}{r_2}, \tag{9}$$

where v_2 is spacecraft's velocity expressed in in Moon-J2000 system, the vector $[x, y, \dot{x}, \dot{y}]$ is the state of the spacecraft in GRC, and ω is the magnitude of the angular velocity $\boldsymbol{\omega}_2$.

Flyby occurs when the spacecraft is less than some set distance from the perturbing planet. In Anderson's [19] study and a NASA report [26], the set distance from the perturbing planet is considered as the sphere of influence and is adopted in this study. Two types of radius of sphere of influence are defined as follows:

$$r_{\text{ROI}} = r_m \left(\frac{\mu_m}{\mu_e} \right)^{2/5}, \tag{10}$$

$$r_{\text{Hill-ROI}} = r_m \left(\frac{\mu_m}{\mu_e} \right)^{1/3}, \tag{11}$$

where r_m denotes the distance between the Earth and the Moon. Considering the ratio of the magnitude of the Moon's perturbing force to that of the Earth-centered two-body force and the ratio of the magnitude of the Earth's perturbing force to that of the Moon-centered two-body force, r_{ROI} denotes the locus of points when these two ratios are equal. In the Earth-Moon system, $r_{\text{ROI}} = 0.1723$ in nondimensional form. It is clear that, within r_{ROI}, the Moon's gravitational influence takes a leading role [26]. $r_{\text{Hill-ROI}}$ is a much broader definition for the sphere of influence, called the Hill radius. Theoretically, a spacecraft outside the Hill radius cannot be captured by the Moon and the Earth's gravitation dominates the gravitational field. In the Earth-Moon system, $r_{\text{Hill-ROI}} = 0.2310$ in nondimensional form.

Therefore, two important criteria are proposed in this study. ***Criterion* I:** the **closest distance** between the spacecraft and the Moon is denoted r_1. If the initial parameters can cause the closest distance to lie within the Moon's sphere of influence r_{ROI}, the Moon's gravitation is certainly powerful enough to affect trajectories, and resonant orbits can lose their steady ratios. We may not able to obtain a resonant orbit using the single-shooting method in the CRTBP given this condition. If the initial parameters can cause the closest distance to lie outside the Moon's sphere of influence r_{ROI} but within the Hill radius $r_{\text{Hill-ROI}}$, we must consider ***Criterion* II:** the **Kepler energy** of the spacecraft with respect to the Moon within a certain region causes the energy E to change significantly. Resonance transition may also occur if the Kepler energy of the spacecraft relative to the Moon labeled by H_2 is temporarily no-positive ($H_2(t) \leq 0$ when $t_1 < t < t_2$, and $H_2(t) > 0$ when $t < t_1$, $t > t_2$).

The closest distance r_1 and the Kepler energy H_2 are simulated as the eccentricity and initial phase are varied. Two representative cases are investigated, including $m > n$ and $m < n$. The numerical integrator adopted is a classic eighth order Runge-Kutta with a seventh order automatic step-size control. The tolerance is defined as 1×10^{-14}.

4.1. 1:2 Resonant Family. We take a 1:2 resonant family as an example in this section. Figure 6 shows all the closest distances for $e \in [0.1, 0.9]$ and $\theta_0 \in [0^\circ, 360^\circ]$ in the 1:2 resonant family.

The dark navy blue area in Figure 6 indicates that the parameters in this area satisfy Criterion I. The closest distances are within the sphere of influence when $r_1 \leq 0.1723$. Within these areas, the Moon's gravitation is powerful enough to influence resonant orbits. Figure 6 shows that the dark navy blue area corresponds to $0.201 \leq e \leq 0.482$ when $\theta_0 = 0$. When the initial phase $\theta_0 = 100^\circ$, the dark navy blue area corresponds to $0.826 \leq e \leq 0.9$.

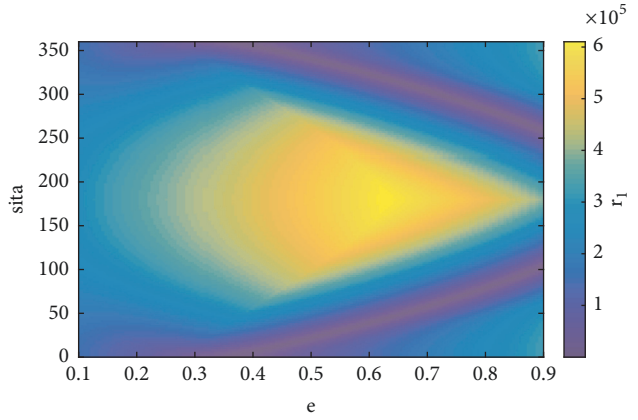

FIGURE 6: Closest distances between the spacecraft and the Moon corresponding to different initial phases and eccentricities for the 1:2 resonant family.

First, we discuss the parameter intervals corresponding to the closest distances within the sphere of influence r_{ROI}. Taking $\theta_0 = 0$ as an example, Figures 7(a) and 7(b) show 1:2 resonant orbits with $0.1 \le e \le 0.9$ in the CRTBP and the two-body problem, respectively. Figure 7(c) shows a partially enlarged view of Figure 7(a) around the Moon. As we can see, compared with the orbits for $\theta_0 = 0$ and $0.1 \le e \le 0.9$ in Figures 7(a) and 7(b), orbits with $\theta_0 = 0$ and $e \in [0.2, 0.5]$ all perform a "loop" in the two-body model and are severely affected by the Moon in the CRTBP. It is worth noting that the results presented in Figure 7 are obtained using the single-shooting method where a single initial condition propagates with constraints being enforced in the final state along this single propagation arc. We always can obtain a corrected closed orbit if the multiple shooting method is used, but the period of this corrected orbit may be quite different from the original period.

We randomly choose a few of cases to verity the proposed criterion when $\theta_0 \neq 0$. Figures 8(a)–8(d) show the J2000 and GRC views of 1:2 resonant orbits with $e = 0.47$ and $\theta_0 = 10^\circ$, which is located in the dark navy area in Figure 6.

In Figure 8, the red trajectory denotes Moon in J2000 and the red point denotes Moon in the rotating frame. The blue and magenta trajectories denote the resonant orbits before and after the second approach to the Moon, respectively. The green and yellow points denote the initial and final integration points, respectively. The black point denotes the Earth. In Figures 8(a)-8(b), it is obvious that temporary capture occurs over a very short time when the orbit approaches the Moon for the first time. The spacecraft subsequently transits into a 5:4 resonant orbit and moves steadily until the second Moon approach. Subsequently, the orbit suddenly transits into the 1:3 resonant orbit, which is shown in Figures 8(c)-8(d). Figure 8(e) shows a partially enlarged view of Figure 8(d). The trajectories in the green and black circles refer to first and second approaches, respectively. The variation in the orbital period during two Moon approaches is shown in Figure 8(f), which were determined based on Chapter 4.4 in Howard [27]. The Moon's period is 2π in nondimensional form. The Moon's period in the 5:4 and 1:3 resonant orbits is 1.6π and 6π, respectively, and is indicated with a red dotted line. We can see the periods in the new orbit after the first and second captures are nearly equal to those in the 5:4 and 1:3 resonant orbits, respectively.

Similarly, we present the 1:2 orbit with $e = 0.85$ and $\theta_0 = 90^\circ$ in Figures 9(a)–9(e). The trajectory transits into the 2:1 resonant orbit after its first Moon approach and then transits into the 1:4 resonant orbit after its second Moon approach. The Moon can cause weak capture, and the spacecraft should be ejected from the Moon and transition into another resonant orbit since the capture is temporary. Figure 9(e) shows a partially enlarged view of Figure 9(d). The trajectory in the green circle refers to the first approach. There is no obvious revolution during the second approach, but we can also see that the trajectory is clearly affected by the Moon after the second approach, which is marked in the black circle in Figure 9(e). The variation of the orbital period during the two Moon approaches is shown in Figure 9(f). It is clear that each transition is trigged by the close approach to the Moon.

Figure 10 shows the 1:2 resonant orbits with $e = 0.7$, $\theta_0 = 60^\circ$. In this case, the closest distance is equal to 0.0397 in nondimensional form. The spacecraft completes a gravity assist maneuver through flyby and escapes from the Earth-Moon system after approaching the Moon. More simulation results regarding the closest distance within the Moon's sphere of influence can be found in Table 1. Since the closest distance distribution is symmetric about $\theta_0 = 180^\circ$, we only listed results from $\theta_0 = 0^\circ$ to 100°.

Resonant orbits with eccentricity and initial phase satisfying Criterion I possess opportunities for a close approach to the Moon; flyby and resonant transition can occur. The simulation results demonstrate the validity of Criterion I; the Moon's gravitation is certainly powerful enough to affect trajectories and resonant orbits can lose their steady ratios when the geometric parameters cause the closest distance to lie within the Moon's sphere of influence r_{ROI}.

Furthermore, we investigate the parameter intervals within the light navy area in Figure 6. Initial parameters in this area can lead to the closest distances of resonant orbits to remain within the Hill radius ($0.1723 \le r_1 \le 0.2310$). The black area in Figure 11 corresponds to parameter intervals satisfying *Criterion* II; the Kepler energy is temporary nonpositive when the closest distance is within the Hill radius and outside r_{ROI}.

It is found that the area corresponding to a temporarily nonpositive Kepler energy shrinks significantly as the eccentricity increases. This result indicates that most resonant orbits with steady ratios generally have large eccentricities, which is consistent with Antoniadou's [17] conclusion.

We perform numerous simulations corresponding to the black area in Figure 11, and the results are summarized in Table 2. Taking the resonant orbit with $e = 0.21$ and $\theta_0 = 10^\circ$ as an example, the closest distance in this condition is 0.23 in nondimensional form, resulting in a temporarily nonpositive Kepler energy of -0.0023. The trajectory performs resonant transitions during the simulation, which are shown in Figures 12(a)–12(f). In Figure 12, the red trajectory denotes the Moon in J2000 and the red point denotes Moon in the rotating frame. The blue and magenta trajectories denote the resonant

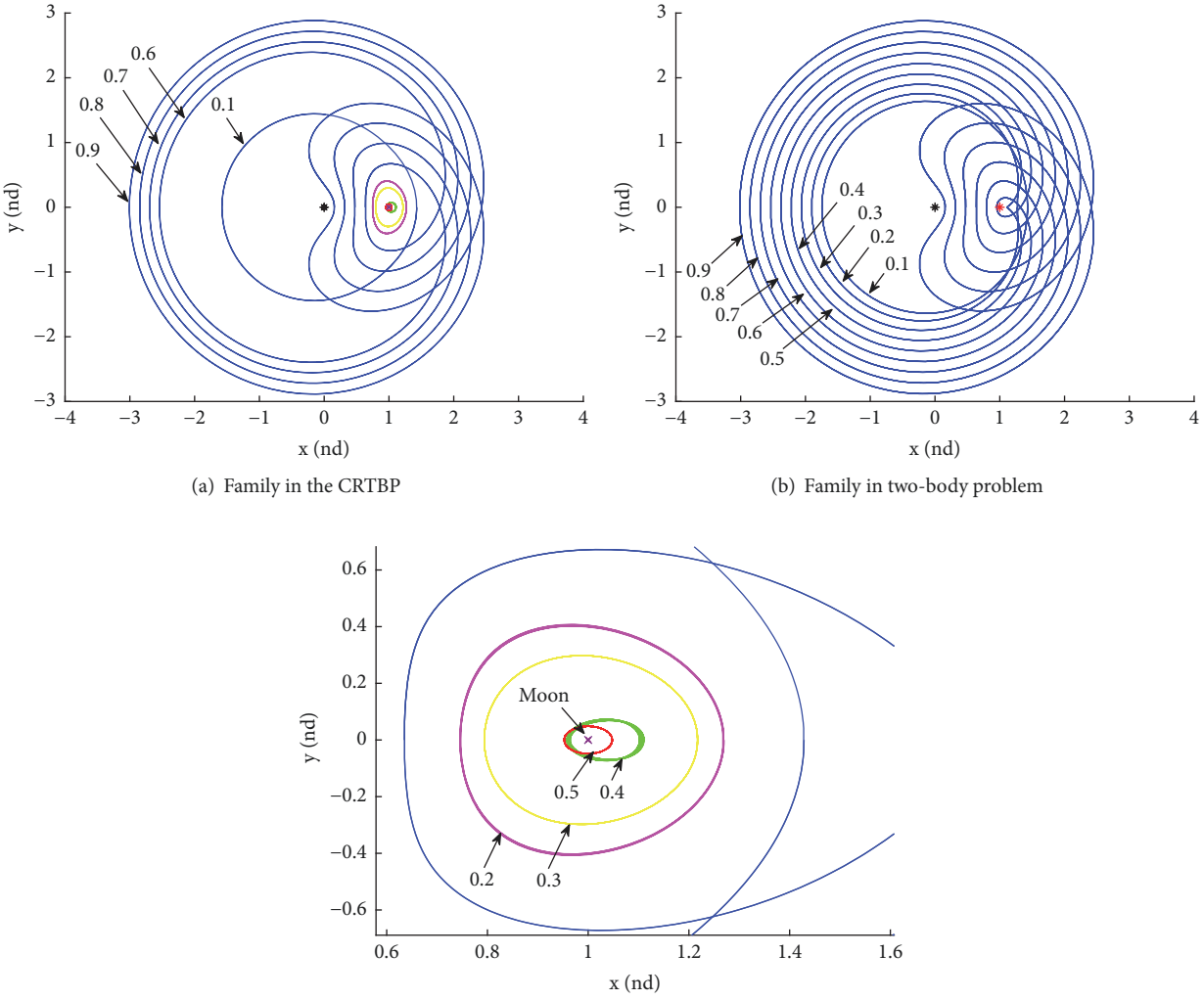

(a) Family in the CRTBP

(b) Family in two-body problem

(c) Partially enlarged view of (a)

FIGURE 7: 1:2 resonant family in the CRTBP and two-body problem.

orbits before and after the first approach but before the second approach to Moon, respectively, while the black trajectory denotes the resonant orbits after the second approach to the Moon. The green and yellow points denote the initial and final integration points, respectively. The black point denotes the Earth. It is clear that the trajectory begins in the 1:2 resonant orbit. After the first Moon approach, the trajectory is suddenly ejected to a 2:1 resonant orbit with much smaller semimajor axis. The process is shown in Figures 12(a)-12(b). We continue integration and find that the trajectory transits to the 1:4 resonant orbit after the second Moon approach, as shown in Figures 12(c)-12(d). Figure 12(e) shows a partially enlarged view of Figure 12(d). The trajectories in the green and black circles refer to first and second approaches, respectively. Variations in the orbital period during the two Moon approaches are shown in Figure 12(f).

Although the closest point on the resonant trajectory is outside the Moon's sphere of influence, Moon's gravitational influence still severely affects the trajectory within the Hill radius where the temporary Kepler energy is nonpositive. Resonance transition also happens in this area.

We also examine parameters corresponding to the case where the closest distance lies within the Hill radius ($0.1723 \leq r_1 \leq 0.2310$) but with positive Kepler energy, as well as parameters corresponding to the case where the closest distance lies outsides the Hill radius. The results are listed in Tables 3 and 4, respectively. Table 4 shows that the resonant orbit can maintain steady ratio when the closest distance is outside the Hill radius. When the closest distance is between r_{ROI} and the Hill radius with positive Kepler energy, most resonant orbits in this area can also maintain a steady ratio. In special cases, when the closest distance is very close to the Hill radius, resonance transition still occurs even with positive Kepler energy, e.g., $\theta_0 = 10$ and $e = 0.57$. These orbits are complicated in the CRTBP when the closest distances are within the Hill radius.

The aforementioned simulation results demonstrate the validity of Criterion II, where resonant orbits can lose their

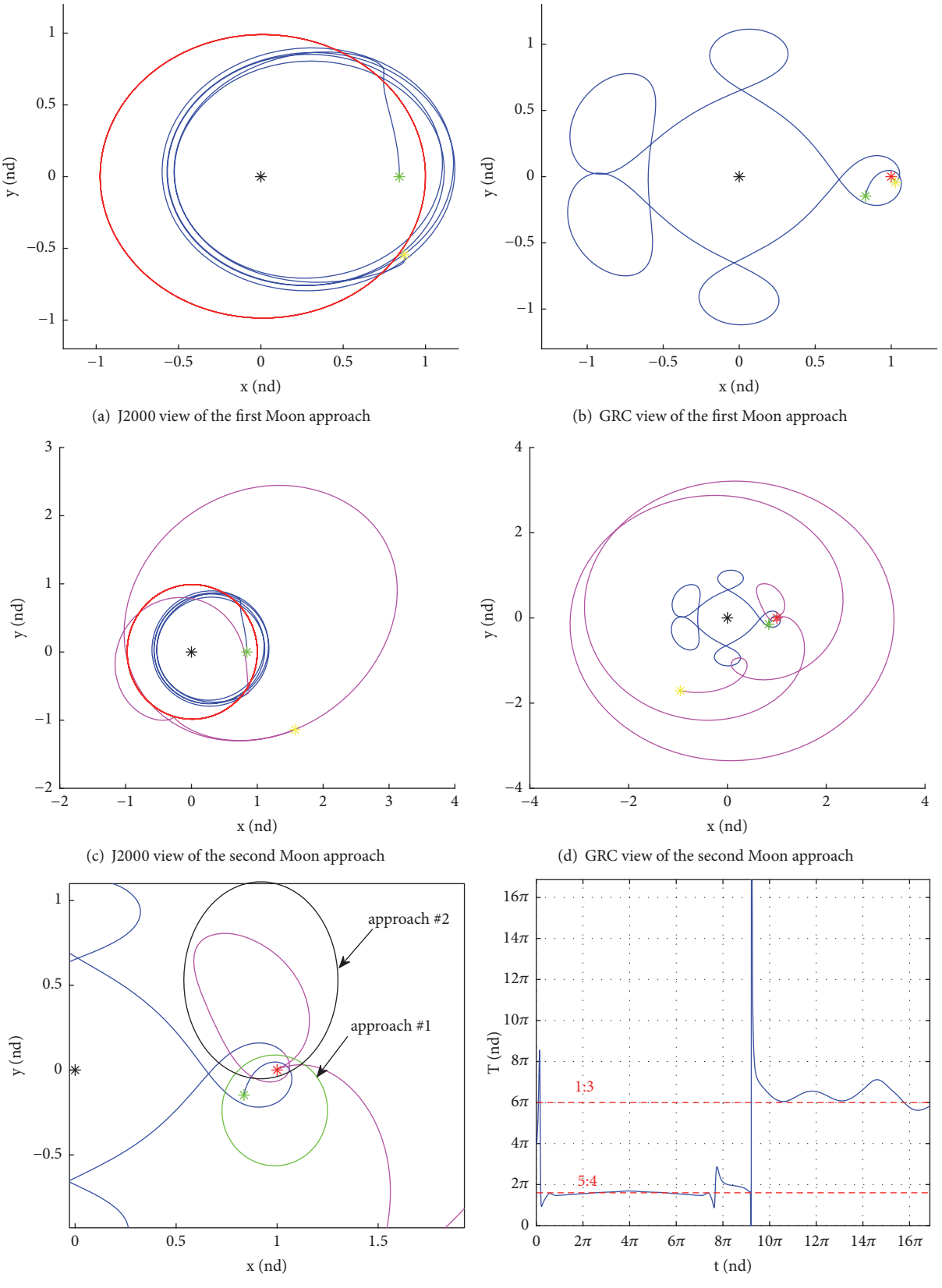

(a) J2000 view of the first Moon approach

(b) GRC view of the first Moon approach

(c) J2000 view of the second Moon approach

(d) GRC view of the second Moon approach

(e) Partially enlarged view of (d)

(f) Variations in the orbital period

Figure 8: Resonance transition and weak capture by the Moon in the 1:2 resonant orbit with $e = 0.47$ and $\theta_0 = 10^\circ$.

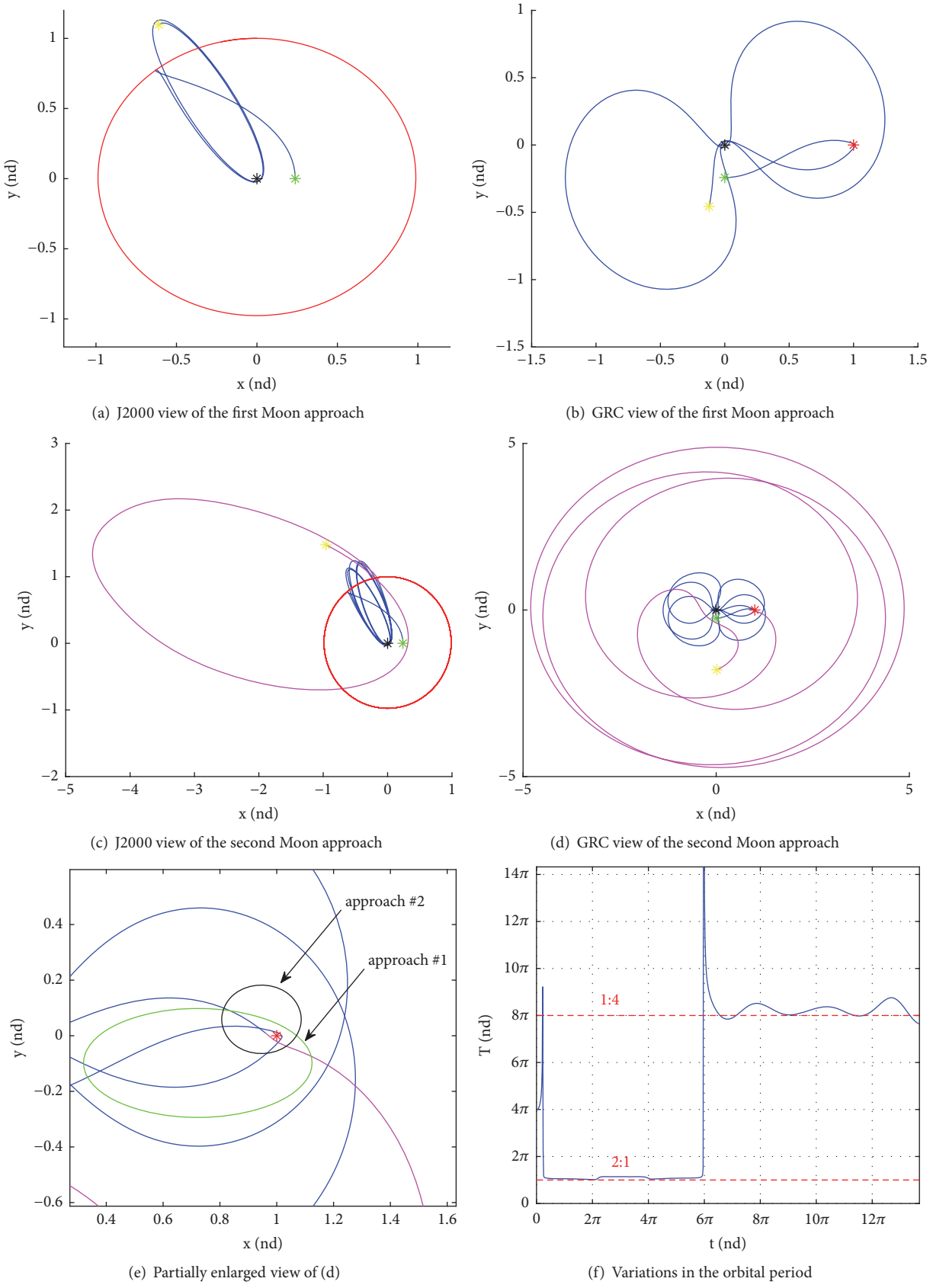

(a) J2000 view of the first Moon approach

(b) GRC view of the first Moon approach

(c) J2000 view of the second Moon approach

(d) GRC view of the second Moon approach

(e) Partially enlarged view of (d)

(f) Variations in the orbital period

FIGURE 9: Resonance transition and weak capture by the Moon in the 1:2 resonant orbit with $e = 0.85$, $\theta_0 = 90^\circ$.

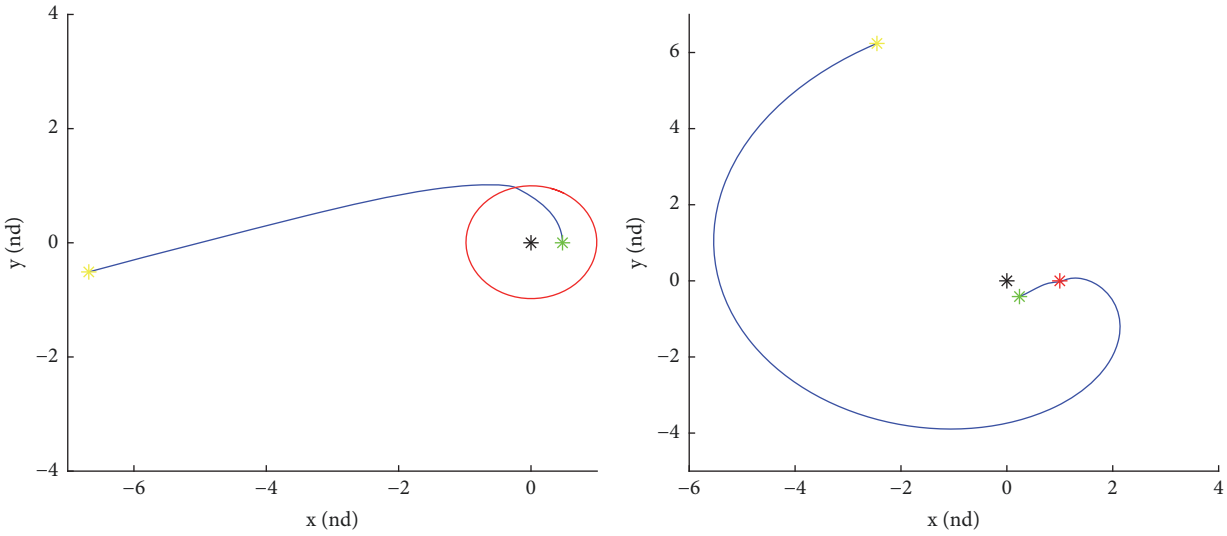

(a) J2000 view (b) GRC view

Figure 10: Flyby in the 1:2 resonant orbit with $e = 0.7$, $\theta_0 = 60^\circ$.

Table 1: Simulation results for the 1:2 resonant orbits when the initial parameters can cause the closest distance to lie within the Moon's sphere of influence.

Initial Phase θ_0	Eccentricity e	Simulation Results
10°	0.34	Flyby
	0.43	Flyby
	0.5	Resonance transition
20°	0.43	Flyby
	0.5	Flyby
	0.55	Resonance transition
30°	0.5	Flyby
	0.54	Flyby
	0.6	Resonance transition
40°	0.56	Flyby
	0.6	Flyby
	0.65	Resonance transition
50°	0.61	Flyby
	0.67	Flyby
	0.71	Resonance transition
60°	0.67	Resonance transition
	0.71	Flyby
	0.75	Resonance transition
70°	0.72	Resonance transition
	0.76	Flyby
	0.8	Resonance transition
80°	0.76	Resonance transition
	0.8	Flyby
	0.84	Resonance transition
90°	0.81	Resonance transition
	0.84	Flyby
	0.88	Resonance transition
100°	---	---
	---	---
	---	---

Table 2: Simulation results for 1:2 resonant orbits when the initial parameters define the closest distance as $r_{\text{ROI}} \le r_1 \le r_{\text{Hill-ROI}}$ and temporary Kepler energy $H_2 \le 0$.

Initial Phase θ_0	Eccentricity e	Closest Distances r_1	Kepler Energy H_2	Simulation Results
5°	0.26	0.1908	-0.0636	Resonance transition
	0.485	0.1715	-0.0033	Resonance transition
10°	0.26	0.2303	-0.0489	Resonance transition
	0.32	0.1961	-0.0587	Resonance transition
15°	0.36	0.2210	-0.0360	Resonance transition
	0.38	0.1821	-0.0325	Resonance transition
20°	0.41	0.2033	-0.0111	Resonance transition

Table 3: Simulation results for 1:2 resonant orbits when the initial parameters can cause closest distance $r_{\text{ROI}} \le r_1 \le r_{\text{Hill-ROI}}$ and temporary Kepler energy $H_2 > 0$.

Initial Phase θ_0	Eccentricity e	Closest Distances r_1	Kepler Energy H_2	Simulation Results
10°	0.51	0.1859	0.0314	Steady ratio
	0.57	0.17235 very close to Hill radius	0.0418	Resonance transition
20°	0.56	0.1916	0.0957	Steady ratio
	0.59	0.17241 very close to Hill radius	0.1080	Resonance transition
30°	0.48	0.2007	0.0339	Steady ratio
	0.62	0.2133	0.1887	Steady ratio
40°	0.55	0.0973	0.0961	Steady ratio
	0.67	0.2059	0.3012	Steady ratio
50°	0.6	0.1955	0.1622	Steady ratio
	0.72	0.2035	0.4688	Steady ratio
60°	0.66	0.1744	0.2798	Steady ratio
	0.77	0.2092	0.7341	Steady ratio
70°	0.71	0.1761	0.4323	Steady ratio
	0.82	0.2253	0.8058	Steady ratio
80°	0.75	0.2039	0.6146	Steady ratio
	0.86	0.2146	0.7649	Steady ratio
90°	0.8	0.1868	0.8001	Steady ratio
	0.9	0.2179	0.7204	Steady ratio

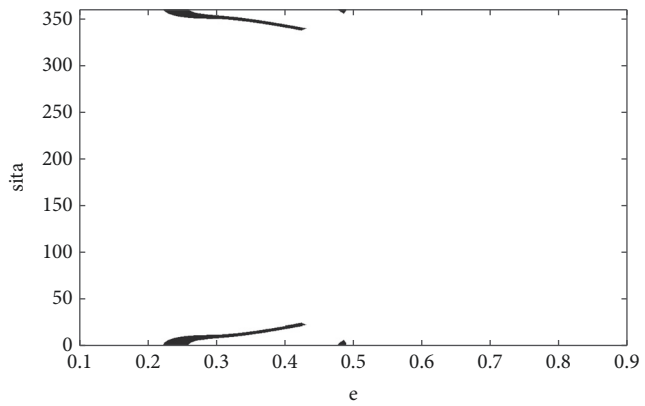

Figure 11: Initial phase and eccentricity values corresponding to temporarily nonpositive Kepler energy in the 1:2 resonant family.

steady ratios as long as the closest distance satisfies $r_{\text{ROI}} \le r_1 \le r_{\text{Hill-ROI}}$ and the temporary Kepler energy $H_2 \le 0$.

4.2. 2:1 Resonant Family. We take the 2:1 resonant family as an example in this section. Figure 13 shows all the closest distances for $e \in [0.1, 0.9]$ and $\theta_0 \in [0^\circ, 360^\circ]$ for the 2:1 resonant family. The dark navy blue area in Figure 13 indicates parameter intervals satisfying Criterion I where the closest distances are within the sphere of influence. Compared with the 1:2 family, the dark navy area is much smaller, which means there are fewer opportunities to approach the Moon. The entire family is far from the Moon when $\theta_0 = 0$, as shown in Figure 5(e). Correspondingly, the closest distance is completely outside the Moon's sphere of influence in Figure 13. The closest distance distribution is symmetric about θ_0=90°, 180°, and 270° when $\theta_0 \neq 0$. The results are understandable and are consistent with the conclusion offered in Section 3. The orbital family in Figure 5(e) will rotate clockwise by θ_0 as θ_0 increases. Compared with Figure 5(e), the orbital family "lies down" when $\theta_0 = 90^\circ$ and 270°, i.e., the possibility of flybys, captures, and resonant transitions is maximized. Numerical simulations about the initial parameters that bring the closest distance within the Moon's sphere of influence are listed in Table 5. Since the closest distance distribution is

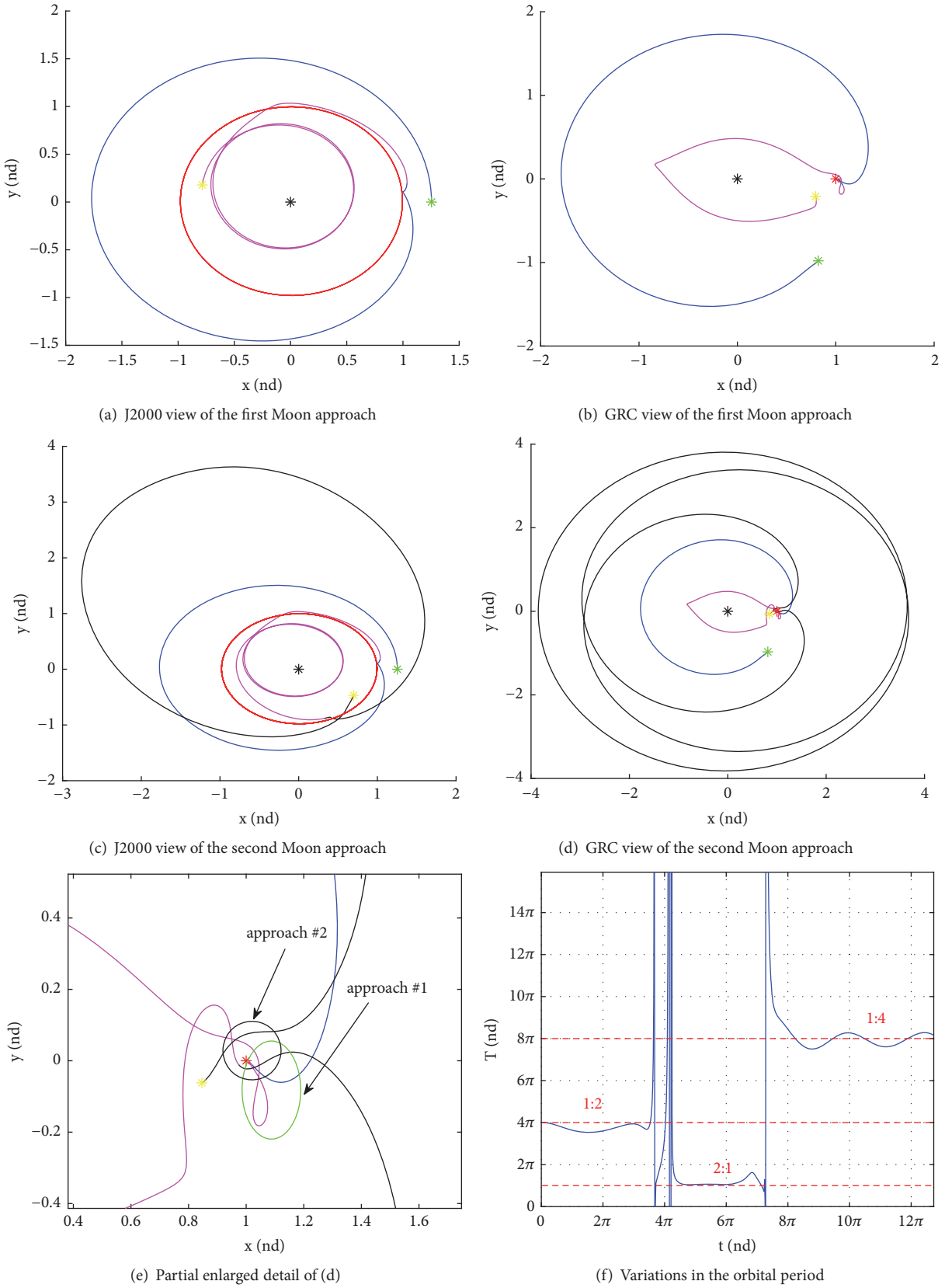

(a) J2000 view of the first Moon approach

(b) GRC view of the first Moon approach

(c) J2000 view of the second Moon approach

(d) GRC view of the second Moon approach

(e) Partial enlarged detail of (d)

(f) Variations in the orbital period

FIGURE 12: Resonance transition and weak capture by the Moon in the 1:2 resonant orbit with $e = 0.21$, $\theta_0 = 10^\circ$.

Table 4: Simulation results for 1:2 resonant orbits when the initial parameters cause closest distance $r_1 > r_{\text{Hill-ROI}}$.

Initial Phase θ_0	Eccentricity e	Simulation Results
10°	0.11	Steady ratio
20°	0.23	Steady ratio
30°	0.11	Steady ratio
40°	0.11	Steady ratio
50°	0.11	Steady ratio
60°	0.11	Steady ratio
70°	0.11	Steady ratio
	0.21	Steady ratio
80°	0.11	Steady ratio
	0.21	Steady ratio
90°	0.21	Steady ratio
	0.33	Steady ratio
100°	0.22	Steady ratio
	0.33	Steady ratio
110°	0.12	Steady ratio
	0.22	Steady ratio
120°	0.12	Steady ratio
	0.21	Steady ratio
	0.32	Steady ratio
130°	0.12	Steady ratio
	0.21	Steady ratio
140°	0.13	Steady ratio
	0.32	Steady ratio
150°	0.13	Steady ratio
	0.32	Steady ratio
160°	0.13	Steady ratio
	0.32	Steady ratio
170°	0.13	Steady ratio
	0.32	Steady ratio
180°	0.13	Steady ratio
	0.32	Steady ratio
--	--	--

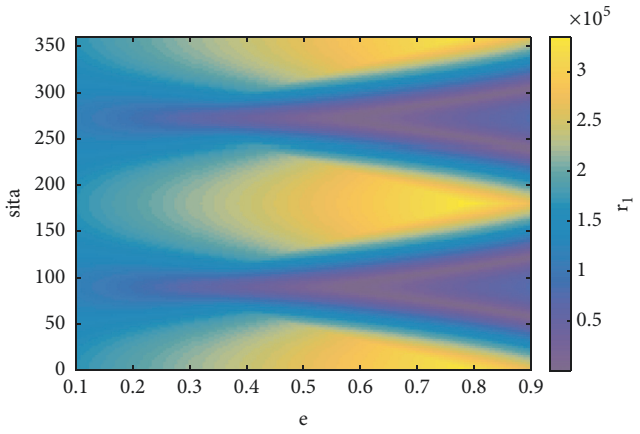

Figure 13: Closest distances corresponding to different initial phase and eccentricity values for 2:1 resonant family.

symmetric about $\theta_0 = 90°$ and 270°, we only list results from $\theta_0 = 50°$ to 90°. The simulations and analysis presented about Figure 13 and Table 5 verify the validity of Criterion I.

The 2:1 resonant family is very special; there are no parameter intervals satisfying Criterion II, where the closest distance is within the Hill radius but without r_{ROI}, and the Kepler energy is temporary nonpositive. Criterion II is unsuitable for the 2:1 resonant family.

5. Conclusion

Some initial parameter values, such as the eccentricity and initial phase, cannot result in resonant orbits in the PCRTBP. This paper presents an analysis of the closest points and Kepler energy of the resonant orbits with respect to Moon that result from different eccentricity and initial phase values. The parameter intervals that allow flyby or weak capture are obtained.

Table 5: Simulation results for 2:1 resonant orbits when the initial parameters can cause the closest distance to lie within the Moon's sphere of influence.

Initial Phase	Eccentricity	Simulation Results
50°	0.85	Resonance transition
	0.9	Flyby
60°	0.75	Resonance transition
	0.83	Resonance transition
	0.88	Flyby
70°	0.61	Resonance transition
	0.7	Resonance transition
	0.78	Flyby
	0.87	Resonance transition
80°	0.45	Resonance transition
	0.57	Resonance transition
	0.66	Flyby
	0.79	Resonance transition
90°	0.89	Resonance transition
	0.33	Resonance transition
	0.43	Resonance transition
	0.58	Resonance transition
	0.7	Resonance transition

When the resonant orbits only satisfy Criterion I, where the closest distance is within the Moon's sphere of influence, the spacecraft has opportunities to closely approach the Moon. Flyby and resonant transition can occur in these conditions. Resonance transition and weak capture can occur when the parameter intervals cause the closest distance to lie within the Hill radius but outside r_{ROI}, and the Kepler energy is temporary nonpositive, resonance transition and weak capture can happen. If the closest distance is relatively large and is outside the Hill radius, resonant orbits can maintain steady resonant ratios.

Examples of the resonant orbit in 1:2 exterior resonance and 2:1 interior resonance respectively are examined to verify the proposed criteria. This analysis will benefit trajectory design in a real mission. Other resonant families can be analyzed in a similar manner. Research on resonant orbits and their related resonance flybys and transitions can provide an alternative option for trajectory design and potentially reduce propellant requirements.

Data Availability

The data used to support the findings of this study are available from the corresponding author upon request.

Conflicts of Interest

The authors declare that they have no conflicts of interest.

Acknowledgments

This work is supported in part by the National Natural Science Foundation of China (Projects nos. 11772009 and 11672007).

References

[1] M. Vaquero and K. C. Howell, "Transfer Design Exploiting Resonant Orbits and Manifolds in the Saturn–Titan System," *Journal of Spacecraft and Rockets*, vol. 50, no. 5, pp. 1069–1085, 2013.

[2] C. D. Murray and S. F. Dermott, *Solar System Dynamics*, Cambridge University Press, Cambridge, UK, 1999.

[3] T. A. Michtchenko and S. Ferrez-Mello, "Modeling the 5 : 2 Mean-Motion Resonance in the Jupiter–Saturn Planetary System," *Icarus*, vol. 149, no. 2, pp. 357–374, 2001.

[4] G. W. Marcy, R. P. Butler, D. A. Fischer et al., "A Planet at 5 AU around 55 Cancri," *The Astrophysical Journal*, vol. 581, no. 2, pp. 1375–1388, 2002.

[5] J. Ji, H. Kinoshita, L. Liu, and G. Li, "Could the 55 Cancri planetary system really be in the 3 : 1 mean motion resonance?" *The Astrophysical Journal*, vol. 585, no. 2, pp. L139–L142, 2003.

[6] K. Goździewski and A. J. Maciejewski, "Dynamical Analysis of the Orbital Parameters of the HD 82943 Planetary System," *The Astrophysical Journal*, vol. 563, no. 1, pp. L81–L85, 2001.

[7] K. Gozdziewski, E. Bois, and A. J. Maciejewski, "Global dynamics of the Gliese 876 planetary system," *Monthly Notices of the Royal Astronomical Society*, vol. 332, no. 4, pp. 839–855, 2002.

[8] D. Psychoyos and J. D. Hadjidemetriou, "Dynamics Of 2/1 Resonant Extrasolar Systems Application to HD82943 and GLIESE876," *Celestial Mechanics and Dynamical Astronomy*, vol. 92, no. 1-3, pp. 135–156, 2005.

[9] D. J. Dichmann, R. Lebois, and J. P. Carrico, "Dynamics of Orbits Near 3:1 Resonance in the Earth-Moon System," *The Journal of the Astronautical Sciences*, vol. 60, no. 1, pp. 51–86, 2013.

[10] G. Voyatzis, "Chaos, Order, and Periodic Orbits in 3 : 1 Resonant Planetary Dynamics," *The Astrophysical Journal*, vol. 675, no. 1, pp. 802–816, 2008.

[11] K. I. Antoniadou and G. Voyatzis, "2/1 resonant periodic orbits in three dimensional planetary systems," *Celestial Mechanics and Dynamical Astronomy*, vol. 115, no. 2, pp. 161–184, 2013.

[12] E. W. Brown and C. A. Shook, *Planetary Theory*, Cambridge University Press, UK, 1933.

[13] M. Vaquero and K. C. Howell, "Design of transfer trajectories between resonant orbits in the Earth–Moon restricted problem," *Acta Astronautica*, vol. 94, no. 1, pp. 302–317, 2014.

[14] C. Petrovich, R. Malhotra, and S. Tremaine, "Planets near mean-motion resonances," *The Astrophysical Journal*, vol. 770, no. 1, 2013.

[15] J. J. Lissauer, D. C. Fabrycky, E. B. Ford et al., "A closely packed system of low-mass, low-density planets transiting Kepler-11," *Nature*, vol. 470, no. 7332, pp. 53–58, 2011.

[16] M. Vaquero and K. C. Howell, "Leveraging Resonant-Orbit Manifolds to Design Transfers Between Libration-Point Orbits," *Journal of Guidance, Control, and Dynamics*, vol. 37, no. 4, pp. 1143–1157, 2014.

[17] K. I. Antoniadou and G. Voyatzis, "Resonant periodic orbits in the exoplanetary systems," *Astrophysics and Space Science*, vol. 349, no. 2, pp. 657–676, 2014.

[18] R. L. Anderson, S. Campagnola, and G. Lantoine, "Broad search for unstable resonant orbits in the planar circular restricted three-body problem," *Celestial Mechanics and Dynamical Astronomy*, vol. 124, no. 2, pp. 177–199, 2016.

[19] R. L. Anderson and M. W. Lo, "A Dynamical Systems Analysis of Resonant Flybys: Ballistic Case," *The Journal of the Astronautical Sciences*, vol. 58, no. 2, pp. 167–194, 2011.

[20] W. S. Koon, M. W. Lo, J. E. Marsden, and S. D. Ross, "Heteroclinic connections between periodic orbits and resonance transitions in celestial mechanics," *Chaos*, vol. 10, no. 2, pp. 427–469, 2000.

[21] R. L. Anderson and M. W. Lo, "Dynamical Systems Analysis of Planetary Flybys and Approach: Planar Europa Orbiter," *Journal of Guidance, Control, and Dynamics*, vol. 33, no. 6, pp. 1899–1912, 2010.

[22] P. S. Laplace, *Traité de Mécanique Céleste*, vol. 4, Courcier, Paris, France, 1805.

[23] F. Tisserand, *Traité de la Mécanique Céleste: Théories des Satellites de Jupiter et de Satume Perturbations des Petites Planétes*, vol. 4, Gauthier-Villars, Paris, France, 1896.

[24] E. Belbruno, F. Topputo, and M. Gidea, "Resonance transitions associated to weak capture in the restricted three-body problem," *Advances in Space Research*, vol. 42, no. 8, pp. 1330–1351, 2008.

[25] E. Belbruno and B. G. Marsden, "Resonance Hopping in Comets," *The Astronomical Journal*, vol. 113, no. 4, pp. 1433–1444, 1997.

[26] R. R. Burrows, "He Classical "Sphere-of-Influence"," in *NASA TM X-53485*, NASA, 1966.

[27] C. Howard, *Orbital Mechanics for Engineering Students*, Butterworth-Heinemann Press, 2005.